

SI

**Large variations in both dark- and photoconductivity in nanosheet networks as nanomaterial is varied from MoS<sub>2</sub> to WTe<sub>2</sub>**

Graeme Cunningham,<sup>1</sup> Damien Hanlon,<sup>1</sup> Niall McEvoy,<sup>2</sup> Georg S Duesberg<sup>2</sup> and Jonathan N. Coleman<sup>\*1</sup>

<sup>1</sup>*School of Physics, CRANN and AMBER Research Centres, Trinity College Dublin, University of Dublin, Dublin 2, Ireland*

<sup>2</sup>*School of Chemistry, CRANN and AMBER Research Centres, Trinity College Dublin, University of Dublin, Dublin 2, Ireland*

\*colemaj@tcd.ie

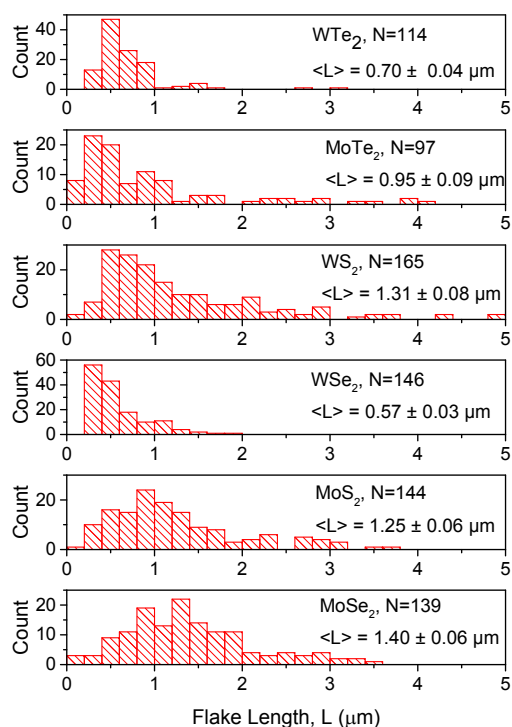


Figure S1: Flake length statistics measured using TEM. The length is defined as the longest dimension of the flake. The quoted errors are standard errors of the distribution. The mean length scales approximately inversely with density suggesting the variation in size occurs during centrifugation.

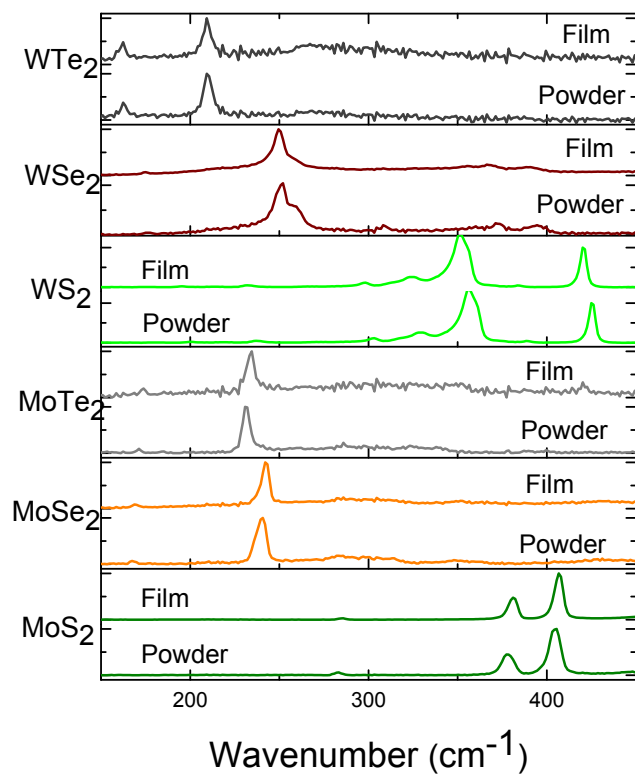


Figure S2: Raman spectra of both powder and films obtained with 532 nm excitation wavelength for all materials studied.

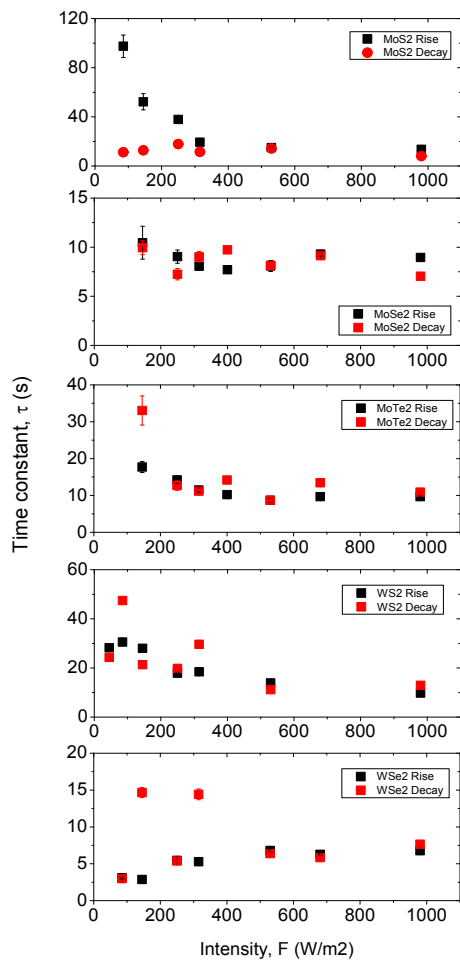


Figure S3: Measured time constants associated with both rise and decay of photocurrent with time for all materials, plotted versus incident intensity.

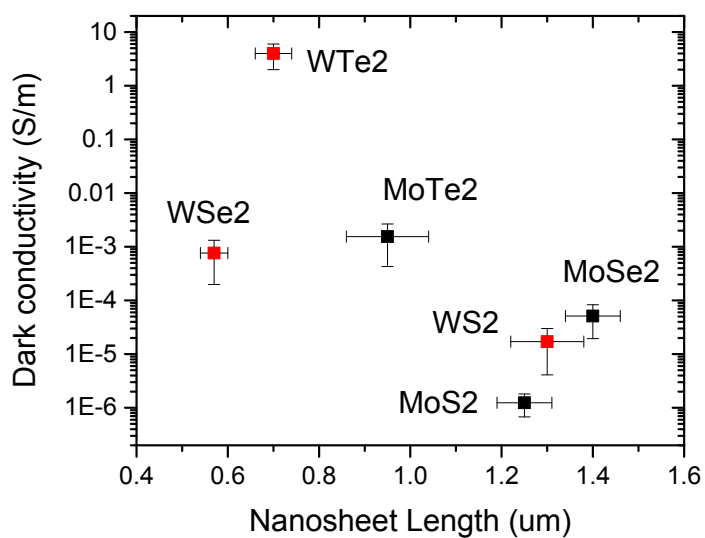


Figure S4: Dark conductivity plotted versus flake length. The apparent reduction in conductivity with increasing flake length is implausible from a physical perspective and is unlikely to be real.

### Bulk Indirect Bandgaps of TMDs

The table below outlines the sources from which we take the bulk indirect bandgaps for the six TMDs studied.

Material	MoS <sub>2</sub>	MoSe <sub>2</sub>	MoTe <sub>2</sub>	WS <sub>2</sub>	WSe <sub>2</sub>	WTe <sub>2</sub>
Values (eV)	1.2 <sup>1,2</sup>	1.1 <sup>1,3</sup>	1.0 <sup>4</sup> , 0.9 <sup>5</sup>	1.3 <sup>1,2</sup>	1.2 <sup>1,3</sup>	0.9 <sup>5</sup> , 0.8 <sup>6</sup>
Value used	1.2	1.1	0.95	1.3	1.2	0.85

It is important to note that although layered and exfoliable, WTe<sub>2</sub> is not a typical Group VI TMD. This material is distinguished by its distorted octahedral co-ordination of the metal atom and is similar in structure to the high temperature  $\beta$ -phase of MoTe<sub>2</sub>.<sup>7-9</sup> The associated reduction in M-M bond length induces a band overlap,<sup>7,8</sup> which is thought to cause WTe<sub>2</sub> to be somewhat metallic<sup>10</sup> or semi-metallic<sup>10-12</sup> and much more conductive than the other group VI TMDs.<sup>10,12</sup> This has been supported by measurements on its Seebeck co-efficient<sup>13</sup> and temperature dependence of resistivity<sup>10</sup> and is in stark contrast to the semiconducting 2H-polytype with trigonal prismatic co-ordination, commonly manifest in the other five regular group VI TMDs.

The little that is known about WTe<sub>2</sub> experimentally comes from older studies on bulk crystals.<sup>7,8,10,13</sup> Whilst its bandstructure has recently been studied computationally along with the other five members of the group VI TMD family, these studies render it hypothetically in the 2H-polytype as a semiconductor with a bulk indirect bandgap of roughly 0.8 eV for consistency.<sup>5,6</sup> This idealisation somewhat confuses matters as such a phase has not been found to exist in practice (at least so far).

However, for presentation purposes, we plot WTe<sub>2</sub> as if it has a bandgap of 0.85 eV as predicted for 2H WTe<sub>2</sub>.

### Schottky barrier analysis of dark current

For a metal semiconductor interface with a Schottky barrier, the current is given by

$$J = A^* T^2 e^{-q\Phi/kT} \left[ e^{qV/kT} - 1 \right]$$

where  $A^*$  is the Richardson constant and  $\Phi$  is the size of the Schottky barrier. In our case we have back to back M-S junctions and so are always in the reverse bias regime. To address this, we consider the slope of the J-V relationship at the origin as this is the same in both forward and reverse bias regimes.

For extremely small voltages, we can expand the exponential to give

$$J = A^* T^2 e^{-q\Phi/kT} qV / kT = \frac{A^* T q}{k} e^{-q\Phi/kT} V$$

We write the barrier height as some fraction of the bandgap:  $\Phi = E_g / c$  where  $c > 1$ . We can then express this as an effective conductivity (i.e. as reported in figure 5A) via

$\sigma = L(dJ / dV)_{V=0}$  where L is the inter-electrode spacing to give:

$$\sigma = \frac{L A^* T q}{k} e^{-qE_g / ckT}$$

This equation can be used to analyse the data in figure 5A. For both types of material, the data is consistent with  $c=1.5$ . This would be consistent with the presence of large Schottky barriers, equal to about 66% of the bandgap are present e.g. ~800 meV for MoS<sub>2</sub>. This is certainly not impossible.

However, this model is inconsistent with the data in certain respects. First, it is unclear why the Schottky barrier should be ~66% of the bandgap for all six materials, especially given they have widely varying conduction and valence band positions,<sup>5</sup> although it may of course be associated with Fermi Level pinning.

In addition, here, the combination  $LA^*Tq / k = 2 \times 10^8$  S/m. This is reasonably close to the value of the intercept in figure 5A for the MoX<sub>2</sub> data ( $9 \times 10^7$  S/m). However, for the WX<sub>2</sub> data, the intercept is considerably higher ( $1.6 \times 10^{10}$  S/m). It is not clear how such a discrepancy should arise within the framework of Schottky barriers.

Thus, while we cannot rule out the presence of Schottky barriers, we believe that the data does not conclusively demonstrate their presence.

<sup>1</sup> Hong Jiang, *The Journal of Physical Chemistry C*, **116**, 2012, 7664.

<sup>2</sup> A. Kuc, N. Zibouche, and T. Heine, *Physical Review B*, **83**, 2011.

<sup>3</sup> Philipp Tonndorf, Robert Schmidt, Philipp Böttger, Xiao Zhang, Janna Börner, Andreas Liebig, Manfred Albrecht, Christian Kloc, Ovidiu Gordan, and Dietrich R. T. Zahn, *Optics Express*, **21**, 2013, 4908.

- 4 Mahito Yamamoto, Sheng Tsung Wang, Meiyang Ni, Yen-Fu Lin, Song-Lin Li, Shinya Aikawa,  
Wen-Bin Jian, Keiji Ueno, Katsunori Wakabayashi, and Kazuhito Tsukagoshi, *ACS Nano*,  
2014.
- 5 Jun Kang, Sefaattin Tongay, Jian Zhou, Jingbo Li, and Junqiao Wu, *Applied Physics Letters*,  
**102**, 2013, 012111.
- 6 A. Kumar and P. K. Ahluwalia, *The European Physical Journal B*, **85**, 2012.
- 7 W. G. Dawson and D. W. Bullett, *Journal of Physics C: Solid State Physics*, **20**, 1987, 6159.
- 8 S.W. Hla, V. Marinkovic, A. Prodan, and I. Musevic, *Surface science*, **352-354**, 1996, 105.
- 9 B. E. Brown, *Acta Crystallographica*, **20**, 1966, 268.
- 10 J. Augustin, V. Eyert, Th Böker, W. Frentrup, H. Dwelk, C. Janowitz, and R. Manzke, *Physical  
Review B*, **62**, 2000, 10812.
- 11 Mazhar N. Ali, Jun Xiong, Steven Flynn, Jing Tao, Quinn D. Gibson, Leslie M. Schoop, Tian  
Liang, Neel Haldolaarachchige, Max Hirschberger, N. P. Ong, and R. J. Cava, *Nature*, 2014.
- 12 J.E. Callanan, G.A. Hope, R.D. Weir, and E.F. Westrum, *J. Chem. Thermodynamics*, **24**, 1992,  
627.
- 13 E. Revolinsky and D. Beerntsen, *Journal of Applied Physics*, **35**, 1964, 2086.